

In vitro heat generation by ferrimagnetic maghemite microspheres for hyperthermic treatment of cancer under an alternating magnetic field

Masakazu Kawashita · Shinjiro Domi · Yasuhiro Saito · Masaaki Aoki ·
Yukihiro Ebisawa · Tadashi Kokubo · Takashi Saito · Mikio Takano ·
Norio Araki · Masahiro Hiraoka

Received: 26 October 2006 / Accepted: 14 August 2007 / Published online: 4 October 2007
© Springer Science+Business Media, LLC 2007

Abstract Ferrimagnetic materials can be expected to be useful as thermo seeds for hyperthermic treatment of cancer, especially where the cancer is located in deep parts of body, as they can generate heat by magnetic hysteretic loss when they are placed in an alternating magnetic field. Recently, it was reported that ferrimagnetic maghemite (γ -Fe₂O₃) microspheres 20–30 μm in diameter prepared in aqueous solution can show excellent heat generating ability. However, these microspheres have many cracks on their surfaces. In this study, the preparation conditions for the microspheres was further optimized in order to obtain

crack-free ferrimagnetic microspheres, and the in vitro heat generation of the obtained microspheres was measured in an agar phantom under an alternating magnetic field. Crack-free γ -Fe₂O₃ microspheres 20–30 μm in diameter were obtained successfully. Their saturation magnetization and coercive force were 68 emu g⁻¹ and 198 Oe, respectively. Their heat generation under an alternating magnetic field of 300 Oe at 100 kHz was estimated to be 42 W g⁻¹. The microspheres showed in vitro heat generation when they were dispersed in an agar phantom and placed under an alternating magnetic field. It is believed that these microspheres may be useful for the in situ hyperthermic treatment of cancer.

M. Kawashita (✉)
Photonics and Electronics Science and Engineering Center,
Graduate School of Engineering, Kyoto University, Nishikyo-ku,
Kyoto 615-8510, Japan
e-mail: kawashita@kuee.kyoto-u.ac.jp

S. Domi · Y. Saito
Technical Research Laboratory, Nippon Sheet Glass Co., Ltd,
Itami-shi, Hyogo 664-8520, Japan

M. Aoki
NEOMAX Co., Ltd, Kishima-gun, Saga 849-2102, Japan

Y. Ebisawa
Sumikin Molycorp, Co., Ltd, Minato, Wakayama 640-8404,
Japan

T. Kokubo
Department of Biomedical Sciences, College of Life and Health
Sciences, Chubu University, Kasugai-shi, Aichi 487-8501, Japan

T. Saito · M. Takano
Institute for Chemical Research, Kyoto University, Uji,
Kyoto 611-0011, Japan

N. Araki · M. Hiraoka
Graduate School of Medicine, Kyoto University, Sakyo-ku,
Kyoto 606-8507, Japan

1 Introduction

Cancer cells are generally destroyed at above 43 °C because of their intrinsic microenvironment including low pH, whereas normal cells are not damaged at even higher temperatures [1, 2]. In addition, tumors are more easily heated than the surrounding normal tissue, as their vascular and nervous systems are poorly developed [3–6]. Therefore, hyperthermia is expected to be a very useful treatment of cancer with minimal side effects [1, 2]. Various techniques for heat delivery, such as treatment with hot water, infrared rays, ultrasound and microwaves have been attempted. However, deep-seated tumors cannot be heated effectively and locally using these techniques. Ferrimagnetic microspheres 20–30 μm in diameter may be useful as thermoseeds for inducing hyperthermia in cancers, especially in tumors located deep inside the body. These spheres are entrapped in the capillary bed of the tumors when they are implanted through blood vessels and can

heat cancers locally by their hysteresis loss when placed in an alternating magnetic field.

So far, glass–ceramics containing lithium ferrite (LiFe_5O_8) in a biocompatible matrix of hematite ($\alpha\text{-Fe}_2\text{O}_3$) and a $\text{SiO}_2\text{-P}_2\text{O}_5$ glassy phase [7–9]; magnetite (Fe_3O_4) in a matrix of β -wollastonite ($\beta\text{-CaSiO}_3$) and a $\text{CaO-SiO}_2\text{-B}_2\text{O}_3\text{-P}_2\text{O}_5$ glassy phase [10–18]; $\alpha\text{-Fe}$ in CaO-SiO_2 glasses [19]; Fe_3O_4 in a B_2O_3 -free $\text{CaO-SiO}_2\text{-P}_2\text{O}_5$ glassy phase [20]; Fe_3O_4 in a $\text{CaO-SiO}_2\text{-B}_2\text{O}_3\text{-P}_2\text{O}_5$ glassy phase [21, 22]; zinc-iron ferrite in a CaO-SiO_2 glassy phase [23]; or Fe_3O_4 in $\text{Na}_2\text{O-CaO-SiO}_2\text{-P}_2\text{O}_5$ glassy phase [24–28] have been developed for this purpose. However, none has been produced in the form of microspheres 20–30 μm in diameter, or has shown high heat generating ability. Ferromagnetic microspheres consisted of maghemite ($\gamma\text{-Fe}_2\text{O}_3$) nano-crystals encapsulated within a coating from polyester of valeric and butyric acids [29–32] were also proposed, but there is fear that the microspheres might deteriorate after a long period under body environment.

Recently, we revealed that ferrimagnetic microspheres 20–30 μm in diameter, in which ferrimagnetic Fe_3O_4 is deposited on silica glass microspheres can be obtained by precipitation from aqueous solution and subsequent heat treatment [33]. The heat generation of the microspheres was estimated to be 41 W g^{-1} , under 300 Oe and 100 kHz. However, they had some cracks on their surfaces. In addition, the in vitro heat generation of the microspheres was not investigated. In this study, we attempted to prepare crack-free ferrimagnetic microspheres by a modified aqueous solution method, and their in vitro heat generation was examined in an agar phantom by placing them under an alternating magnetic field.

2 Experimental procedure

2.1 Preparation of microspheres

An iron-containing solution was prepared by dissolving 8.48 g of iron fluoride (FeF_3 ; Morita Chemical Industries Co., Osaka, Japan) in 0.1% hydrofluoric acid solution (500 ml) in a Teflon beaker. Silica (SiO_2) glass microspheres 10 μm in diameter (0.75 g, 99.9 wt%; Catalysts & Chemicals Industries Co., Kanagawa, Japan) were soaked in the iron-containing solution (500 ml) at 33 °C. Subsequently, 0.5 M boric acid (H_3BO_3) solution (0.83 ml; Sigma-Aldrich, Tokyo, Japan) was dropped into the solution while stirring. After 1 h, the products formed in the solution were recovered by filtration, and heated to 600 °C at a rate of $5 \text{ }^\circ\text{C min}^{-1}$, kept at 600 °C for 1 h, and allowed to cool in an atmosphere of 70 vol% CO_2 gas and 30 vol% H_2 gas.

2.2 Structural analysis of microspheres

The crystalline phases precipitated in the products before and after the heat treatment were characterized by powder X-ray diffraction (XRD; RAD-RC, Rigaku Co., Tokyo, Japan) using the following settings: X-ray source, Ni-filtered $\text{CuK}\alpha$ radiation; X-ray power, 40 kV, 150 mA; scanning rate, $2\theta = 3^\circ\text{min}^{-1}$; and sampling angle, 0.3° . The crystalline phases precipitated in the specimens were identified by referring to data from the Joint Committee on Powder Diffraction Standards. The products after the heat treatment were observed using a field-emission scanning electron microscope (FE-SEM; S-4500, Hitachi Ltd., Tokyo, Japan). The crystallite size of the precipitated crystalline phase was estimated by using a transmission electron microscope (TEM; EM-002B, Topcon, Tokyo, Japan).

2.3 Magnetic properties of microspheres

The saturation magnetization and coercive force of the heat-treated products were measured using a magnetic property measurement system (MPMS-XL, Quantum Design, Tokyo, Japan) under magnetic fields up to 10 kOe at room temperature. The amount of heat generated (P) by the products was calculated from the area of the hysteresis loop under a magnetic field of up to 300 Oe, which is a practically available maximum alternating magnetic field, and by using the following equation [34]:

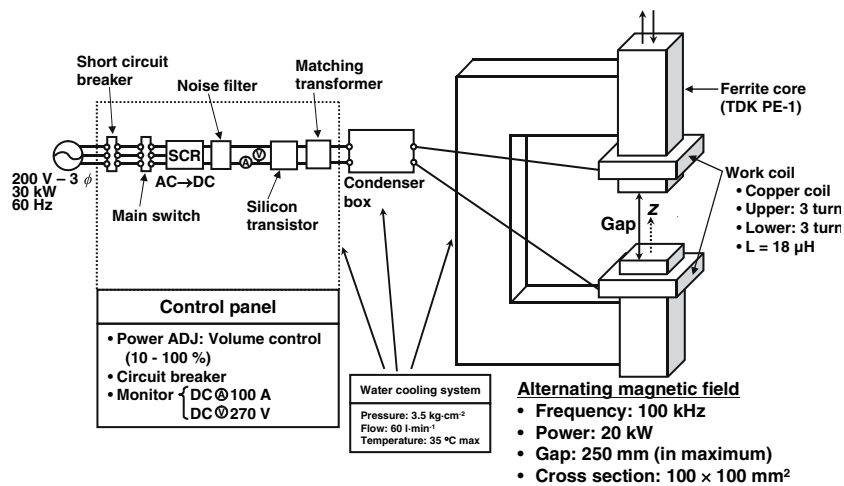
$$P = f \cdot \oint HdB \times 10^{-7}, \quad (1)$$

where f , H and B are the frequency (hertz), the magnetic field strength (oersted) and magnetization (electromagnetic units per gram), respectively.

2.4 Magnetic core-type alternating magnetic field generator

A magnetic core-type alternating magnetic field generator, shown schematically in Fig. 1, was constructed. An electric source was supplied to the silicon controlled rectifier (SCR) bridge. The alternating current was rectified to a direct current and the voltage of the direct current was increased to 270 V through an SCR bridge. After the electric noise was eliminated by the noise filter, the direct current was converted into 100 kHz alternating current through a silicon transistor. Finally, the voltage of the alternating current was raised to 6.42 kV, 422 A through the transformer for matching impedance and the resonance

Fig. 1 Schematic representation of the arrangement of a magnetic core-type alternating magnetic field generator



condenser. The strength of the field could be varied continuously from 10% to 100% by adjusting the voltage of the SCR.

The alternating magnetic field was applied to the gap between the opposite ends of a C-shaped core. The core was made of ferrite (TDK PE-1, Tokyo, Japan) with a cross-section in $100 \times 100 \text{ mm}^2$. Around the each core, a three-turn-copper-solenoid coil with $18 \mu\text{H}$ inductance was settled, via which a 100 kHz alternating electric current was supplied. The gap between opposite cores could be varied from 10 mm to 250 mm by moving the upper core.

Profiles of magnetic field were mapped by the following method. A coil for the measurement of the alternating magnetic field was prepared by coiling a copper wire around a vinyl chloride block with a cross-section area of $20 \times 20 \text{ mm}^2$. The coil was placed at various positions between the opposite cores, connected to an oscilloscope, and then induced electromotive force (V) and frequency (f) were measured when the generator produces an alternating magnetic field. The magnetic field was calculated according to the following equation.

$$B = \frac{V}{2\pi \cdot f \cdot S} \times 10^4, \tag{2}$$

where B , V , f and S are magnetic field (oersted), induced electromotive force (volt), frequency (hertz) and cross-section area of coil (square meter), respectively. The measurement was carried out at the central axial position of the ferrite core.

2.5 Measurement of in vitro heat generation of microspheres

The ferrimagnetic microspheres (10 or 12 mg) were uniformly dispersed into an agar phantom (4 or 6 g) and

placed under an alternating magnetic field generated by the magnetic core-type generator described in Sect. 2.4. Temperature increase in the agar phantom was measured using a fluoroptic thermometer (Model 3000, Luxtron). In some cases, the microspheres were locally distributed at the tip of the fluoroptic thermometer.

3 Results and discussion

3.1 Structure of microspheres

Figure 2 shows the XRD patterns of microspheres as prepared in aqueous solution and those subsequently heat treated in $\text{CO}_2\text{-H}_2$ gas. Peaks assigned to $\beta\text{-FeOOH}$ (No. 13–157) were observed for microspheres as prepared, whereas those assigned to $\gamma\text{-Fe}_2\text{O}_3$ (No. 39–136) were observed after the subsequent heat treatment in $\text{CO}_2\text{-H}_2$

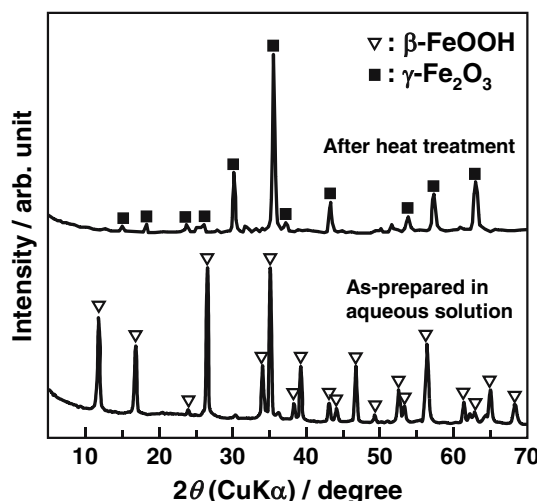


Fig. 2 XRD patterns of the microspheres as prepared in aqueous solution and those subsequently heat treated in $\text{CO}_2\text{-H}_2$ gas

Fig. 3 FE-SEM photographs of the heat-treated products

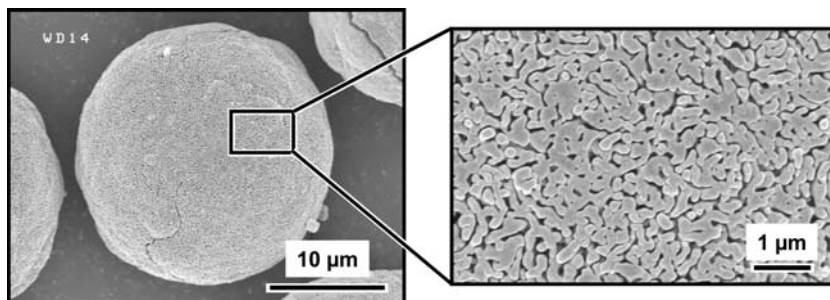
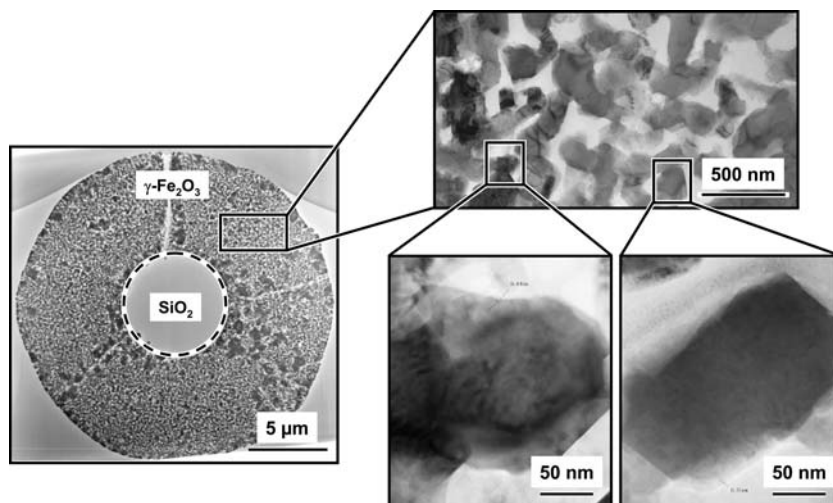


Fig. 4 TEM photographs of a cross-section of the heat-treated products



gas. The absence of the reflections by silica in these patterns indicates that silica microspheres fully covered with $\gamma\text{-Fe}_2\text{O}_3$ can be obtained by the present method. Figure 3 shows the FE-SEM photographs of the obtained products. Spherical and almost crack-free particles approximately 20 μm in diameter were successfully obtained by the present method. It can be seen from Fig. 3 that the surfaces of the specimens were porous, and composed of tiny crystals less than 1 μm in size. These results indicate that the present method gives almost crack-free $\gamma\text{-Fe}_2\text{O}_3$ microspheres with a SiO_2 core approximately of 20 μm in diameter.

Figure 4 shows the TEM photographs of cross-sections of the obtained products. These micrographs show that $\gamma\text{-Fe}_2\text{O}_3$ was deposited uniformly on the surface of SiO_2 glass microspheres. Volume ratio of the $\gamma\text{-Fe}_2\text{O}_3$ crystals to silica glass spheres was estimated to be 30 to 1 from these figures. A total of 70 microspheres were chosen at random and the size of the $\gamma\text{-Fe}_2\text{O}_3$ crystallites was measured by using image analyzing software (analysisIS 3.0, Olympus Soft Imaging System GmbH, Münster, Germany) and a film scanner (LS-4500AF, Nikon, Tokyo, Japan). It was found that $\gamma\text{-Fe}_2\text{O}_3$ had a wide distribution in its crystallite size, as shown in Fig. 5. The average crystallite size of the $\gamma\text{-Fe}_2\text{O}_3$ was estimated at 206 nm. It is considered that the

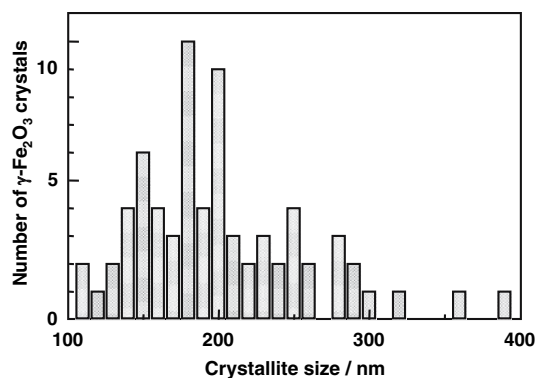
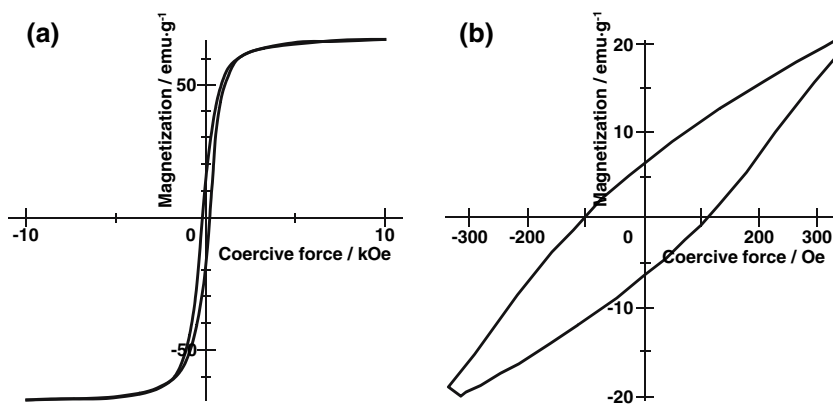


Fig. 5 Crystallite size distribution of $\gamma\text{-Fe}_2\text{O}_3$ precipitated in the heat-treated products

$\gamma\text{-Fe}_2\text{O}_3$ as well as Fe_3O_4 [35] gives a largest coercive force when it has a single domain, since the crystal structure and magnetic properties of $\gamma\text{-Fe}_2\text{O}_3$ are similar to those of Fe_3O_4 . It has been reported that a spherical or cubic $\gamma\text{-Fe}_2\text{O}_3$ particle has a single domain when its crystallite size is smaller than 74 nm [36] or 100 nm [37], respectively. Therefore, the present $\gamma\text{-Fe}_2\text{O}_3$ does not have the optimum crystallite size for high coercive force. It is desirable that the crystallite size of $\gamma\text{-Fe}_2\text{O}_3$ be controlled so that the optimum coercive force is obtained.

Fig. 6 Magnetization curves of the heat-treated products in magnetic fields of up to 10 kOe (a) and up to 300 Oe (b)



3.2 Magnetic properties of microspheres

Figure 6 shows the magnetization curves for the heat-treated products in fields of 10 kOe (a) and 300 Oe (b). It can be seen from Fig. 6(a) that the heat-treated products gave a saturation magnetization of 68 emu g^{-1} and a coercive force of 198 Oe. The heat generation was calculated from the area of the magnetization curves under a magnetic field of 300 Oe given in Fig. 6(b), using Eq. (1), where the frequency (f) was set at 100 kHz. Its value was estimated to be 42 W g^{-1} in 300 Oe at 100 kHz.

3.3 Magnetic field produced by magnetic core-type alternating magnetic field generator

Figure 7 shows the change in magnetic field at a distance (z) from the surface of the bottom ferrite core of 10 mm (i.e. $z = 10 \text{ mm}$) when the gap between ferrite cores is changed. The magnetic field rapidly decreased from 480 to 200 Oe when the gap was increased from 10 to 80 mm. When the gap was larger than 80 mm, the magnetic field

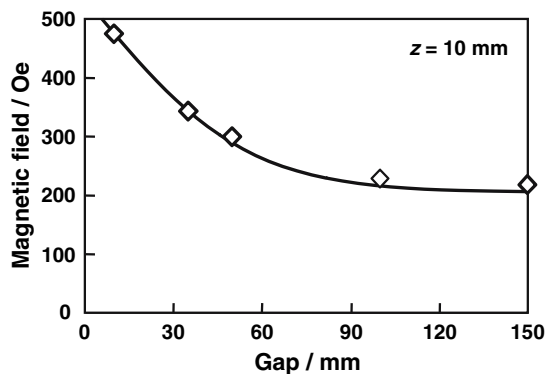


Fig. 7 Change in magnetic field at the distance from the surface of the bottom ferrite core of 10 mm (i.e. $z = 10 \text{ mm}$) as a function of gap between ferrite cores

became constant at approximately 200 Oe. When the present microspheres are clinically used for treatment of deep-seated cancer such as liver cancer, the patient’s stomach is placed between the magnetic cores of the magnetic field generator during the treatment. Therefore, it is considered that a large gap such as 300 mm will be required for clinical application on the assumption that even the largish stomach of the patient can be placed between the magnetic cores. However, the present result indicates that a large magnetic field such as 300 Oe cannot be obtained by the present alternating magnetic field generator, when the gap is large enough for clinical application.

Figure 8 shows the magnetic field as a function of z with gaps of 50 mm (a) and 150 mm (b). When the gap was 50 mm, a uniform and large magnetic field of 300 Oe was obtained despite increasing z . However, when the gap was 150 mm, the magnetic field decreased remarkably with increasing z up to half the length of the gap. These results indicate that the gap should be decreased to 50 mm to obtain a uniform and large magnetic field of 300 Oe in the present alternating magnetic field generator.

3.4 In vitro heat generation of microspheres

Figure 9 shows the change in temperature of 6 g of an agar phantom in which 12 mg of the microspheres were locally distributed at the fiber tip of the fluoroptic thermometer (a) or uniformly distributed (b). The gap and z were set at 30 and 15 mm, respectively. The period of application of alternating magnetic field was set at 10 min. The temperature of the agar phantom rapidly increased within 2 min for the local distribution of the microspheres (see Fig. 9a), whereas it gradually increased for the uniform distribution (see Fig. 9b). The maximum temperature increases for local distribution and uniform distribution were 20 and $2 \text{ }^\circ\text{C}$, respectively. These results indicate that the density of

Fig. 8 Magnetic field as a function of z under the gap of 50 mm (a) and 150 mm (b)

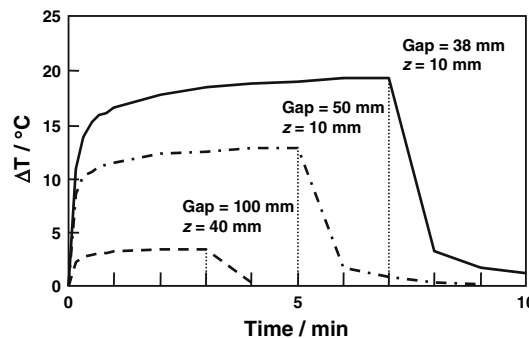
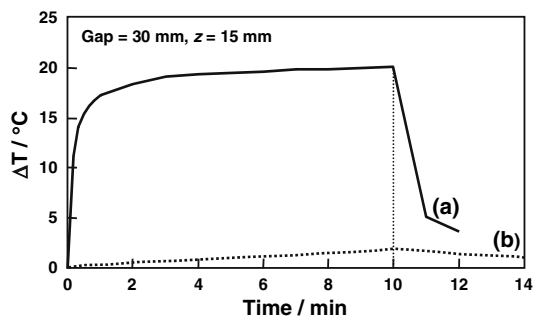
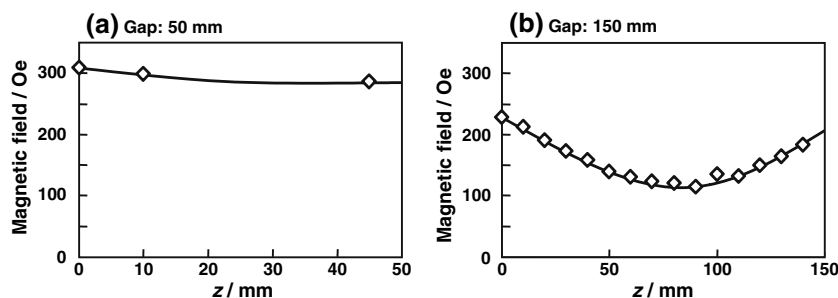


Fig. 9 Change in temperature of the agar phantom in which the microspheres were locally distributed at the fiber tip of the fluoroptic thermometer (a) or uniformly distributed (b)

Fig. 10 Change in temperature of the agar phantom in which the microspheres were locally distributed at the fiber tip of the fluoroptic thermometer, under various gaps and distances z

the microspheres has a large effect on the heat efficacy of the surrounding agar phantom, which indicates that the microspheres should be localized as much as possible for the effective hyperthermic treatment of cancer.

Figure 10 shows the change in temperature of 4 g of an agar phantom in which 10 mg of the microspheres were locally distributed at the fiber tip of the fluoroptic thermometer, under various gaps and distances z . When z was constant at 10 mm, a smaller gap of 38 mm gave a more rapid temperature increase than a larger gap of 50 mm. This is attributed to the higher magnetic field for the smaller gap than for the larger gap, as shown in Figs. 7 and 8. However, when the gap and z were 100 and 40 mm, respectively, the temperature increase was only 3 °C. These findings indicate that a remarkable temperature increase can be obtained if the microspheres are localized and the gap is set below 50 mm. When the gap was 50 mm, the magnetic field was 300 Oe as shown in Fig. 8a. This indicates that the present microspheres can generate a large heat enough for hyperthermic treatment under the magnetic field of 300 Oe. However, the gap should be at least 300 mm for clinical application. Therefore, the heat generation of the microspheres should be further increased by optimizing the composition, controlling the crystallite size of ferrimagnetic crystal and increasing the content of ferrimagnetic crystal, as well as increasing the available magnetic field of the magnetic field generator.

4 Conclusions

Crack-free ferrimagnetic γ - Fe_2O_3 microspheres 20–30 μm in diameter were successfully obtained by optimizing preparation conditions. Their saturated magnetization and coercive force were 68 emu g^{-1} and 198 Oe, respectively. Their heat generation in an alternating magnetic field of 300 Oe at 100 kHz was estimated to be 42 W g^{-1} . The microspheres showed in vitro heat generation when they were dispersed in an agar phantom and placed under an alternating magnetic field. For clinical application, it is desirable that the heat generation of the microspheres be further increased by optimizing the composition, controlling the crystallite size of ferrimagnetic crystal and increasing the content of ferrimagnetic crystal, as well as by increasing the available magnetic field of the magnetic field generator.

Acknowledgments This work was supported in part by a Grant-in-Aid for Scientific Research, the Ministry of Education, Culture, Sports, Science and Technology, Japan and Nanotechnology Support Project of the Ministry of Education, Culture, Sports, Science and Technology, Japan.

References

1. J. CONWAY and A. P. ANDERSON, *Clin. Phys. Physiol. Meas.* 7 (1986) 287

2. T. SUGIHARA, “Gan-to-Tatakau-Hyperthermia (Japanese)”, (Kyoto, Kinpoudou, 1986) p. 37–48
3. R. CAVALIERE, E. C CIOCATTO, B. C GIOVANELLA, C. HEIDELBERGER, R. O JOHNSON, M. MARGOTTINI, B. MONDOVI, G. MORICCA and A. ROSSI-FANELLI, *Cancer* **20** (1967) 1351
4. K. OVERGAARD and J. OVERGAARD, *Eur. J. Cancer* **8** (1972) 65
5. K. OVERGAARD and J. OVERGAARD, *Eur. J. Cancer* **8** (1972) 573
6. J. OVERGAARD, *Cancer* **39** (1977) 2637
7. N. F. BORRELLI, A. A LUDERER, J. N PANZARINO and H. L. RITTLER, *Am. Ceram. Soc. Bull.* **61** (1982) 819
8. A. A. LUDERER, N. F BORRELLI, J. N PANZARINO, G. R. MANSFIELD, D. M HESS, J. L BROWN, E. H BARNETT and E. W HAHN, *Radiat. Res.* **94** (1983) 190
9. N. F. BORRELLI, A. A LUDERER and J. N PANZARINO, *Phys. Med. Biol.* **29** (1984) 487
10. T. KOKUBO, Y. EBISAWA, Y. SUGIMOTO, M. KIYAMA, K. OHURA, T. YAMAMURO, M. HIRAOKA, M. ABE, In “Bioceramics Vol. 3”, edited by J. E. HULBERT and S. F. HULBERT (Rose-Hulman Institute of Technology, Indiana, 1992) p. 213
11. Y. EBISAWA, Y. SUGIMOTO, T. HAYASHI, T. KOKUBO, K. OHURA and T. YAMAMURO, *J. Ceram. Soc. Japan.* **99** (1991) 7
12. Y. EBISAWA, T. KOKUBO, K. OHURA and T. YAMAMURO, *J. Mater. Sci. Mater. Med.* **1** (1990) 239
13. Y. EBISAWA, T. KOKUBO, K. OHURA and T. YAMAMURO, *J. Mater. Sci. Mater. Med.* **4** (1993) 225
14. K. OHURA, M. IKENAGA, T. NAKAMURA, T. YAMAMURO, Y. EBISAWA, T. KOKUBO, Y. KOTOURA and M. OKA, *J. Appl. Biomater.* **2** (1991) 153
15. M. IKENAGA, K. OHURA, T. NAKAMURA, Y. KOTOURA, T. YAMAMURO, M. OKA, Y. EBISAWA, T. KOKUBO, in “Bioceramics Vol. 4”, edited by W. BONFIELD, G. W. HASTINGS and K. E. TANNER (Butterworth–Heinemann Ltd, Oxford, 1991) p. 255
16. M. IKENAGA, K. OHURA, T. YAMAMURO, Y. KOTOURA, M. OKA and T. KOKUBO, *J. Orthop. Res.* **11** (1993) 849
17. Y. EBISAWA, F. MIYAJI, T. KOKUBO, K. OHURA and T. NAKAMURA, *J. Ceram. Soc. Japan* **105** (1997) 947
18. Y. EBISAWA, F. MIYAJI, T. KOKUBO, K. OHURA and T. NAKAMURA, *Biomaterials* **18** (1977) 1277
19. H. KONAKA, F. MIYAJI and T. KOKUBO, *J. Ceram. Soc. Japan* **105** (1997) 833
20. M. KAWASHITA, H. TAKAOKA, T. KOKUBO, T. YAO, S. HAMADA and T. SHINJO, *J. Ceram. Soc. Japan* **109** (2001) 39
21. S. H. OH, S. Y. CHOI, Y. K. LEE and K. N. KIM, *J. Biomed. Mater. Res.* **54** (2001) 360
22. Y. K. LEE, S. B LEE, Y. U KIM, K. N KIM, S. Y CHOI, K. H LEE, I. B SHIM and C. S KIM, *J. Mater. Sci.* **38** (2003) 4221
23. M. KAWASHITA, Y. IWAHASHI, T. KOKUBO, T. YAO, S. HAMADA and T. SHINJO, *J. Ceram. Soc. Japan* **112** (2004) 373
24. O. BRETCANU, S. SPRIANO, E. VERNE, M. COISSON, P. TIBERTO and P. ALLIA, *Acta. Biomater.* **1** (2005) 421
25. T. LEVENTOURI, A. C KIS, J. R THOMPSON and I. M ANDERSON, *Biomaterials* **26** (2005) 4924
26. O. BRETCANU, S. SPRIANO, C. B VITALE and E. VERNE, *J. Mater. Sci.* **41** (2006) 1029
27. O. BRETCANU, E. VERNE, M. COISSON, P. TIBERTO and P. ALLIA, *J. Magn. Magn. Mater.* **300** (2006) 412
28. O. BRETCANU, E. VERNE, M. COISSON, P. TIBERTO and P. ALLIA, *J. Magn. Magn. Mater.* **305** (2006) 529
29. P. MOROZ, S. K. JONES, J. WINTER and B. N. GRAY, *J. Surg. Oncol.* **78** (2001) 22
30. P. MOROZ, S. K JONES and B. N GRAY, *J. Surg. Oncol.* **80** (2002) 149
31. P. MOROZ, S. K JONES, C. METCALF and B. N GRAY, *Int. J. Hypertherm.* **19** (2003) 23
32. N. TSAFNAT, G. TSAFNAT, T. D LAMBERT and S. K JONES, *Phys. Med. Biol.* **50** (2005) 2937
33. M. KAWASHITA, M. TANAKA, T. KOKUBO, T. YAO, S. HAMADA and T. SHINJO, *Biomaterials* **26** (2005) 2231
34. A. Y. MATLOUBIEH, R. B ROEMER and T. C CEATS, *IEEE Trans. Biomed. Eng.* **32** (1984) 227
35. J. E. KNOWLES, *J. Magn. Magn. Mater.* **25** (1981) 105
36. A. AHARONI, *IEEE Trans. Magn.* **22** (1986) 478
37. Y. D. YAN and E. DELLA TORRE, *IEEE Trans. Magn.* **25** (1989) 2919